JOURNAL OF THERMOPHYSICS AND HEAT TRANSFER
Vol. 16, No. 2, April–June 2002

Experimental Investigation of an Air Microjet Array Impingement Cooling Device

John E. Leland* and Rengasamy Ponnappan†
U.S. Air Force Research Laboratory, Wright–Patterson Air Force Base, Ohio 45433-7251
and
Kevin S. Klasing‡
Universal Energy Systems, Inc., Dayton, Ohio 45432–1894

A microjet impingement cooling device for high power electronics was constructed from silicon wafers using microelectromechnical systems fabrication techniques. The array of 221, 0.277-mm-diam jets was tested using air as the coolant for jet diameter Reynolds numbers from 4.65×10^2 to 1.405×10^3. Heat transfer and pressure drop data were obtained for a range of mass rates extending up to the point of choked flow and also for variable heat fluxes. The results were compared to an existing Nusselt correlation for jet impingement arrays that was found to significantly under-predict the heat transfer. A new correlation is provided that also accounts for variable air properties.

Nomenclature

A	=	area
A_f	=	free area ratio, the ratio of total jet area to heat transfer area, $\pi d^2/4x_n^2$
c	=	speed of sound, $\sqrt{(\gamma RT_f)}$
c_p	=	constant pressure specific heat
d	=	jet diameter
G	=	mass flow
h	=	heat transfer coefficient
k	=	thermal conductivity
L	=	heated length
Nu_d	=	average Nusselt number, hd/k
P	=	pressure
Pr	=	Prandtl number, $\mu c_p/k$
q	=	heat flux
R	=	gas constant
Re_d	=	Reynolds number, $\rho U d/\mu$
r	=	recovery factor
T_f	=	film temperature, $(T_i + T_w)/2$
T_i	=	inlet static temperature
T_w	=	average wall temperature
U	=	bulk velocity
V	=	volumetric flow rate
x_n	=	jet-to-jet spacing
z_n	=	jet-to-target spacing
γ	=	ratio of specific heats
θ_{w-f}	=	wall to fluid (at T_i) thermal resistance
μ	=	dynamic viscosity
ρ	=	density

Subscripts

amb	=	ambient
aw	=	adiabatic wall
e	=	exit
i	=	inlet
meas	=	measured
0	=	stagnation

Presented as Paper 99-0476 at the AIAA 37th Aerospace Sciences Meeting, Reno, NV, 11–14 January 1999; received 14 December 2000; revision received 7 December 2001; accepted for publication 3 January 2002.

*Senior Research Engineer, Power Division; currently Director, Technology Partnerships, University of Dayton Research Institute, Dayton, OH 45469-0102. Associate Fellow AIAA.

†Senior Research Engineer, Power Division, Energy Storage & Thermal Science Branch, 1950 Fifth Street, Building 18. Associate Fellow AIAA.

‡Engineer, 4401 Dayton-Xenia Road; currently Lead Engineer, General Electric Aircraft Engines, Turbine Airfoils Center of Excellence, One Neumann Way MD A406, Cincinnati, OH, 45215-1915.

Introduction

THE cooling of high-power electronics is becoming increasingly important to the U.S. Air Force (AF) and commercial industry as the power capacity of devices such as the insulated gate bipolar transistor increase. Some devices being developed by the military have projected waste heat flux levels in excess of 300 W/cm^2. The AF is further interested in employing air cooling where possible. Although a poor heat transfer fluid, air has many advantages. There are no logistics issues, no inventory problems, no environmental concerns, no safety issues, and no special training associated with the use or handling of air. Thus, the use of a different fluid, especially one not already employed by the AF, would come at great cost.[1]

In an effort to meet the demanding cooling requirements of high-power electronics devices and the cost objectives of the AF, a silicon-based microjet array cooler has been built and tested. Ideally, a silicon-based cooler could eventually be machined directly into the die of an electronic device thereby eliminating many thermal resistances and, consequently, making the most of air cooling. An emerging microelectromechnical systems (MEMS) fabrication technique, deep-ion etching, was exploited to machine the fine flow passages within the cooler.

The cooler design incorporates an array of jets impinging on an enhanced surface to achieve high heat transfer rates. Jet impingement heat transfer is known for its ease of implementation and high heat transfer coefficients. It has been employed for the drying of paper and textiles, tempering glass, bearing cooling, turbine blade cooling, and electronics cooling. Many excellent surveys have been performed for air jet impingement,[2–4] which cover hundreds of references. Even with this impressive depth and breadth of literature available, there is very little in the way of data for arrays of very small jets.

Kercher and Tabakoff[5] are perhaps the only investigators to have studied arrays of small diameter jets. Their data cover the ranges $0.25 \le d \le 2.0$ mm, $3.1 \le x_n/d \le 12.5$, $1.0 \le z_n/d \le 4.8$, $0.005 \le A_f \le 0.080$, and $3 \times 10^2 \le Re_d \le 3 \times 10^4$. The array area was 50.8 mm square for all cases. In comparison, the current device

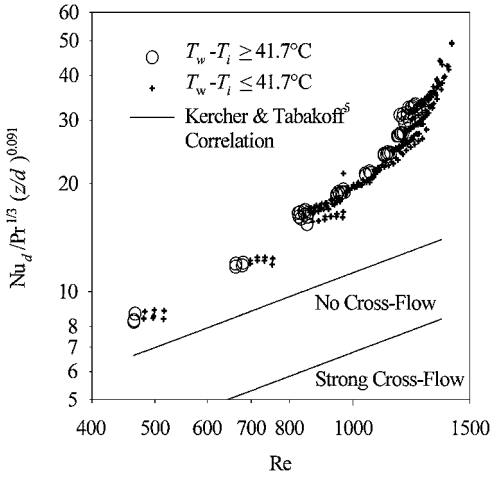

Fig. 1 Comparison of current data to existing correlation.

results are for $d = 0.277$ mm, $x_n/d = 4.44$, 0.96, $A_f = 0.040$, and $4.65 \times 10^2 \leq Re_d \leq 1.405 \times 10^3$. The current array impingement area is 18.2 mm square with a total device footprint of 22.2 mm square. Kercher and Tabakoff made several important conclusions with regard to the array performance: 1) The heat transfer coefficient increases with A_f. 2) The heat transfer coefficient is dominated by Reynolds number Re_d and x_n/d. 3) For constant total jet area, the heat transfer coefficient increases with increasing number of jets. 4) The heat transfer coefficient increases with increasing z_n/d if there is no crossflow, but decreases with increasing z_n/d if crossflow is present. 5) Heat transfer decreases with increasing crossflow. Crossflow is simply the flow traveling perpendicular to the impinging jets. The jets farthest from the center experience the most crossflow. Kercher and Tabakoff correlated their results with the following complex expression:

$$Nu_{d,x} = \phi_1 \phi_2 Re_d^m Pr^{\frac{1}{3}} (z_n/d)^{0.091} \tag{1}$$

where $m = f(x_n/d, Re_d)$, $\phi_1 = f(x_n/d, Re_d)$, and

$$\phi_2 = f\left[\frac{G(X, I-1)}{G(H, I)}, \left(\frac{z_n}{d}\right), Re_d\right]$$

are all evaluated graphically from figures contained within Ref. 5. The term $G(X, I-1)/G(H, I)$ is the ratio of crossflow entering unit area I over the total jet flow for the same unit area. Figure 1 shows the present data compared to Eq. (1) for no crossflow and strong crossflow. The performance of the microjet cooler is substantially better than the best case, no crossflow, predicted by Eq. (1). Thus, there is great promise for this heat transfer concept, but there is also a need for a better understanding of heat transfer and fluid flow in small jet arrays.

Experimental Apparatus

The experimental apparatus consists primarily of the microjet array cooler and the flow and measurement equipment.

Microjet Cooler

The overall objective of the microjet cooler design was to obtain a very compact, high-performance cooler using air as the cooling medium. The complexity of Eq. (1) almost precludes using it as a design tool. As a consequence, the cooler design began with the qualitative conclusions of Kercher and Tabakoff[5] and the limitations of the MEMS deep-ion fabrication technique, the available thickness of silicon wafers (400 μm) and the number of wafers that could be bonded into a stack (four). The wafer thickness established the jet-to-target spacing z_n, which then set the range of optimal jet diameters. From there, several iterations of Eq. (1) established the jet spacing and other parameters. The microjet cooler is constructed from four, 400-μm deep-ion etched silicon wafers to form a plenum, jet array

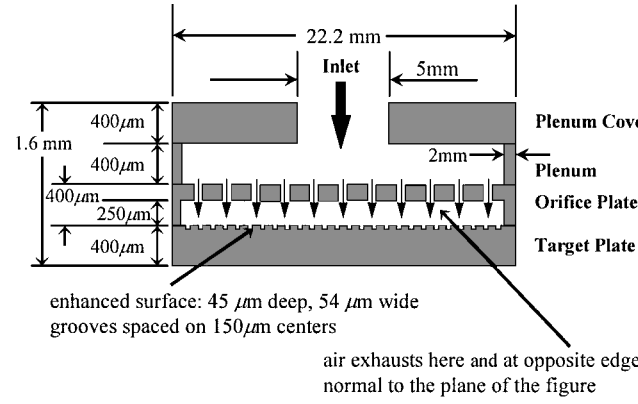

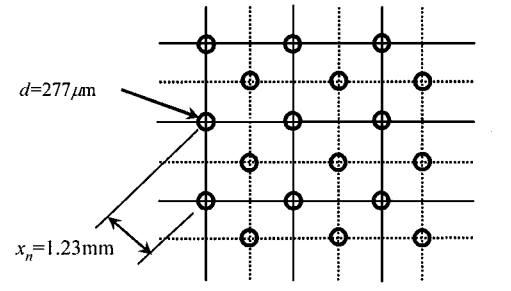

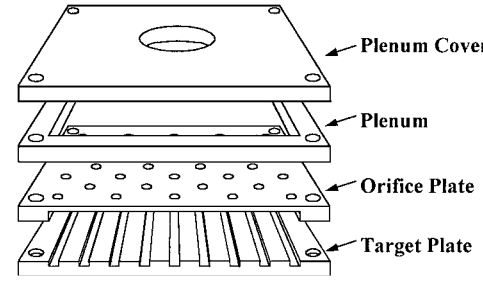

Fig. 2 Schematic of microjet array cooler.

or orifice plate, and heat transfer surface or target plate. Figure 2 shows a schematic of the cooler. Air enters the device plenum and is distributed over the orifice plate. The air then flows through the orifice plate creating a high heat transfer zone under each of the 221 jets. The air is then exhausted from two opposing edges of the cooler, normal to the plane of the cross section shown in Fig. 2.

The primary limitations of this type of construction are the wafer thickness and the inability to bond more than four wafers. Thus, the wafer thickness is the dominant driver in the design. The literature shows that, for a single jet, heat transfer is optimal for $2 \leq z_n/d \leq 4$ with orifice-type nozzles. The optimal spacing is related to the length of the potential core and velocity profile of the jet, the latter being primarily a function of nozzle type and nozzle entry geometry. Above this range, heat transfer is reduced with increasing z_n/d. Below this range, heat transfer is less effected, and a secondary maximum may occur when confined jet conditions, $z_n/d = 0.25$, are approached. Note that the preceding observations have been made for single jets and that Kercher and Tabakoff[5] did not note an optimal z_n/d for their jet arrays. However, Kercher and Tabakoff found that larger z_n/d caused reduced heat transfer in the presence of crossflow. Thus, to obtain good heat transfer and to satisfy deep-ion etch hole fabrication limitations, $z_n/d \approx 1$ was chosen, which yielded a jet diameter of 250 μm. (An actual hole size of 277 μm resulted.) Given d, the correlation of Kercher and Tabakoff indicated that $4 \lesssim x_n/d \lesssim 5$ would yield good results for the assumed Reynolds number regime.

The total jet area was then used to define the inlet area. At 5 mm in diameter, the inlet hole area is substantially larger than the total

jet area. Unfortunately, wafer thickness and fabrication limitations caused the flow area in the plenum to be slightly restricted at the point where the inlet flow impinges the lower plenum plate and is turned radially outward. It was later found that this had much more severe implications than first surmised. As will be discussed later, the restriction led to recirculating flows in the plenum and above the target plate that created a ring of reduced jet flow onto the target plate.

The described configuration yields a value of A_f that is more than seven times greater in the present experiments than the highest value studied by Kercher and Tabakoff[5] for a similar jet diameter. To compensate for the large value of A_f, the target plate was constructed with 45 μm deep by 54 μm wide grooves on 152-μm centers. The addition of widely spaced shallow grooves increases the heat transfer area while minimizing any effect on flow distribution. This change reduces the ratio of A_f to target plate area to one that is closer to that studied by Kercher and Tabakoff for the subject jet diameter. Note that the jet diameter is more than six times the groove width and that the jet-to-target plate spacing is taken as an area weighted average to account for the grooves. Details of the device are shown in Fig. 2.

Flow and Measurement System

A schematic of the flow and measurement system is shown in Fig. 3. Other details of the measurement system are shown in Fig. 4. Shop air at 1.2 MPa is filtered, dried, and then regulated to achieve the desired volumetric flow rate. The inlet flow static pressure is measured by a calibrated pressure transducer. The inlet temperature measured by a 1.59-mm probe type-T thermocouple is corrected by the following equation:

$$T_i = T_{\text{meas}} - r\left(U^2/2c_p\right) \tag{2}$$

where the recovery factor is defined as $r = Pr^m$ and $m = 0.84$ for laminar flow and $m = 0.89$ for turbulent flow. A rotameter, or variable area flow meter, is used to obtain the volumetric flow rate, which is corrected for off standard temperature and pressure by the following equation:

$$V = V_{\text{meas}}\sqrt{(T_R/T_i)(P_i/P_R)} \tag{3}$$

where T_R and P_R are standard temperature and pressure, respectively. When it is realized

$$V = U_i/A_i \tag{4}$$

Eqs. (2–4) may be combined to obtain T_i.

Heat is applied to the microjet array cooler by four resistance-matched, thick-film resistors soldered directly to a copper heat spreader. Thermal grease was used to minimize the thermal resistance between the copper heat spreader and the microjet array cooler. The heaters and microjet array cooler were well insulated with low thermal conductivity, 0.3 W/mK, Glastherm HT (General Electric Corporation) and Fiberfrax (Carborundum Company). Figure 5 shows the locations of 14 type-T 30 American Wire Gage (AWG) thermocouples which were embedded in 0.69-mm holes drilled along the midplane of a 2.31-mm-thick copper heat spreader. The area weighted average of these temperatures T_w and the adiabatic wall temperature were used to calculate the average heat transfer coefficient:

$$h = q/(T_w - T_{i,\text{aw}}) \tag{5}$$

The temperature drop through the copper and silicon is considered small, and by not accounting for it, a more conservative estimate of the heat transfer coefficient is obtained. The heat flux is obtained by subtracting the heat loss from the electrical power into the resistors. A correction was made for the difference in area between the target plate and resistive heaters. The heat loss was obtained as a function of T_w by applying power to the heaters with zero airflow. An additional set of experiments with zero power input and various flow rates showed that viscous heating was negligible.

A pitot tube constructed from 26 gauge hypodermic tubing, 0.25 mm i.d., was used to measure the stagnation pressure of the exit air as shown in Fig. 4. The pitot tube was maintained at a distance of 1.5 mm, less than eight planar exit jet hydraulic diameters, from the

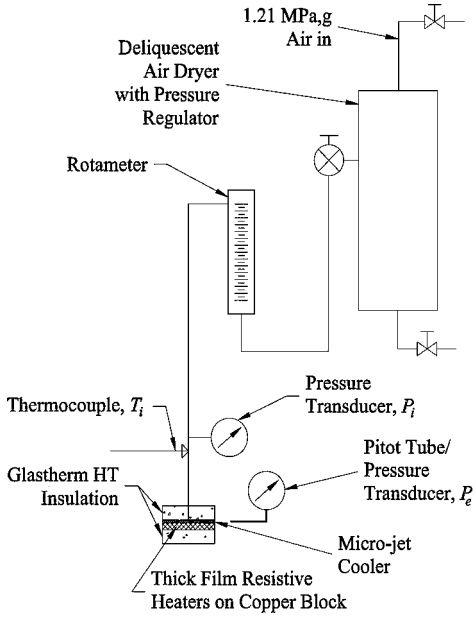

Fig. 3 Flow and measurement system schematic.

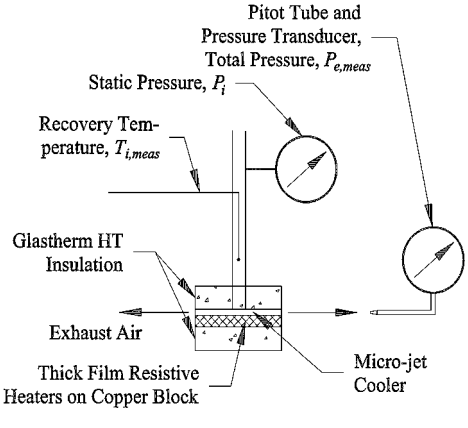

Fig. 4 Schematic of microjet array cooler and measurement system.

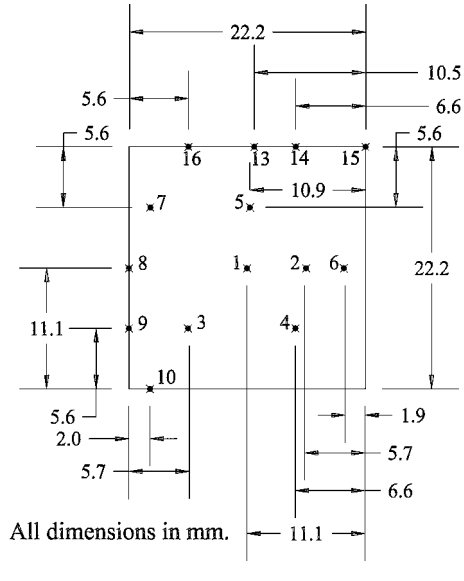

Fig. 5 Schematic of thermocouple locations.

plane of the exiting jet. Pressure measurements were taken along the length of the exiting jet for each flow rate, and the exit profile was determined to be flat, indicating that the flow was well distributed at the exit. A type-T 30 AWG thermocouple mounted near the pitot tube was used to measure the exit air temperature. The exit velocity was obtained by

$$U_e = \sqrt{2c_0^2 - 2c_0\sqrt{c_0^2 - [2(P_{0,e} - P_{\text{amb}})/\rho_0]}} \tag{6}$$

where c_0 is evaluated at the exit stagnation temperature $T_{0,e}$. This equation accounts for compressibility effects. The exit stagnation temperature is determined from

$$T_{0,e} = T_{\text{meas}} + (1 - r)\left(U_e^2 \big/ 2c_p\right) \tag{7}$$

The exit velocity may be found by the simultaneous solution of Eqs. (6) and (7). The exit temperature may then be obtained from Eq. (2).

The experiments were performed by setting the volumetric flow rate and then incrementing the heat input until the device reached the predetermined limit of 80°C. The 80°C limit was imposed because the glue used to bond the silicon wafers was limited to 85°C in operating capability. The inlet temperature was not controlled but was observed to remain nearly constant during each experiment. The inlet temperature ranged only from 20.6 to 23.3°C over the entire range of data. All properties were calculated at the film temperature unless otherwise noted.

Uncertainty Analysis

A Hewlett Packard 3852A data acquisition system was used to make all voltage and temperature measurements. This device has a resolution of 0.02°C and rated accuracies of 0.65°C for T-type thermocouples. The data acquisition unit and type-T thermocouples were compared to a precision digital resistance temperature device (0.03°C rated accuracy), over the range of interest, and the system accuracy was found to actually be within 0.3°C. All type-T thermocouples were found to agree with each other to within 0.1°C for the entire temperature range of interest.

The heat flux was calculated from the measurement of the voltage and current into the thick-film resistors. The standard Kline and McClintock[6] approach to random uncertainty calculation yields an uncertainty of 0.27% in the electrical power input. Heat loss was determined by applying power to the resistors with zero flow through the microjet array cooler. The heat loss was then correlated as a function of T_w and subtracted from the electrical power input at a given T_w. The percent heat loss was the greatest for low air mass flow rates and low-power inputs and was the smallest for the converse. For example, the heat loss was about 15% for 0.5 g/s airflow and less than 4% for 3.7 g/s.

The uncertainty of the pressure measurements was 5 Pa. The uncertainty of the mass flow rate calculation was dominated by the uncertainty of the flow meter, which was 3% of the reading. The repeatability of the data was generally within 2% for heat fluxes greater than 2 W/cm^2. A minimum of two runs were made for each flow rate. Finally, the bias error was not estimated.

Results

Results were obtained for a range of input pressures that yielded flow rates near the lower limit of the flow meter capability to choked flow at the exit of the microjet array cooler. The jet diameter Reynolds number ranged from 4.65×10^3 to 1.405×10^4 under these conditions. The device average heat transfer coefficient was obtained for a variety of heat fluxes to determine the effect of variable properties of the air. A Nusselt correlation including a correction for variable properties was developed.

Figure 6 shows how the heat flux varies with the device pressure drop for two values of T_w. As may be seen, the heat flux values level out and become unsteady after choked flow occurs at the exit plane of the device, indicative of a converging nozzle. Power electronics case temperatures in excess of 85°C are not uncommon for military applications. One can easily see that heat fluxes greater than 15 W/cm^2 are possible for these higher case temperatures.

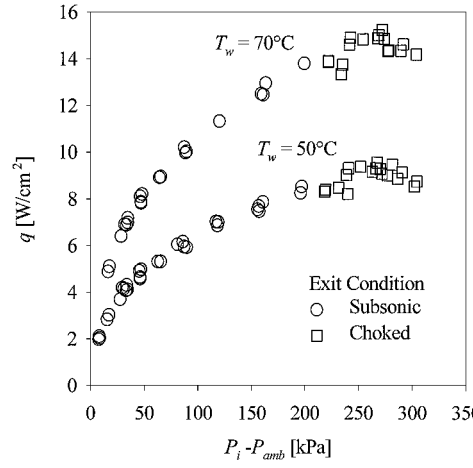

Fig. 6 Heat flux vs pressure drop.

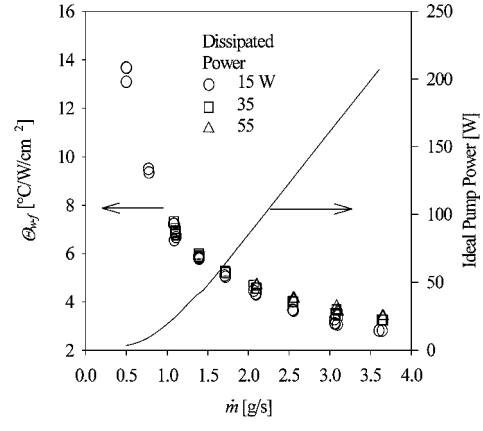

Fig. 7 Thermal resistance vs mass flow rate.

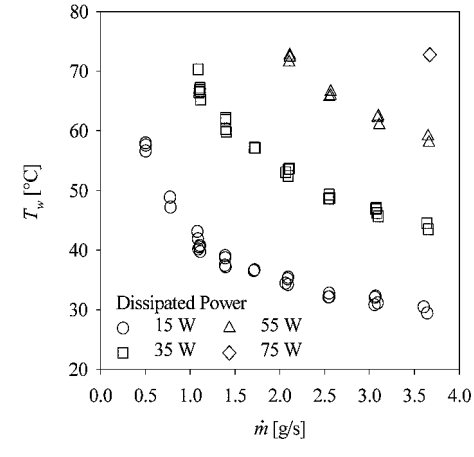

Fig. 8 Wall temperature vs mass flow rate.

The effect of mass flow on the device thermal resistance θ_{w-f} may be seen in Fig. 7. For an air-cooled heat sink, the performance of the microjet array is impressive, <14°C/W/cm^2. State-of-the-art commercially available pin fin heat sinks with integral muffin fans[7] have thermal resistances ranging from 28 to 185°C/W/cm^2. In fact, the performance of the microjet array is comparable to commercially available liquid-cooled cold plates. However, this has a price. Figure 7 also shows that achieving this level of performance with an air-cooled heat sink comes with a significant estimated pump power cost.

For the electronics cooling designer, Fig. 8 shows the mass flow rate that would be required to maintain a desired operating

temperature for various power inputs. As with the device thermal resistance, it may be seen that there are diminishing returns for increasing the flow rate.

The data are compared to the correlation developed by Kercher and Tabakoff,[5] Eq. (1), in Fig. 1. Figure 1 clearly shows that the performance of the microjet array is substantially better than that obtained for by Kercher and Tabakoff for their arrays. As stated earlier, the geometric and test parameters of the current microjet array device are within the ranges studied by Kercher and Tabakoff. However, for the jet diameter used in the present experiments, x_n and z_n are both smaller than the range covered by Kercher and Tabakoff. Furthermore, although the increased area of the target plate has been adjusted for, the shallow grooves may enhance heat transfer in other ways. This combination of factors explains why the performance of the current device is underpredicted. Kercher and Tabakoff found that decreased x_n increases the free area A_f, which increases heat transfer. For nearly the same jet diameter as used by Kercher and Tabakoff, A_f is more than seven times greater in the present experiments. Furthermore, Kercher and Tabakoff found that under conditions of crossflow, decreased z_n/d also increases heat transfer.

In the present experiments, the parameter z_n/d is about half the smallest value studied by Kercher and Tabakoff[5] for the same nozzle diameter. In a companion numerical effort following the experiments described herein, Selvam et al.[8] showed that reducing z_n/d from 1.5 to 0.96 yielded a heat transfer increase of about 2% and that further reducing z_n/d from 0.96 to 0.5 yielded an additional increase of 9%. The numerical results indicate that the trend identified by Kercher and Tabakoff,[5] that the heat transfer coefficient increases with decreasing z_n/d if crossflow is present, is valid for smaller values of z_n/d. The results of Kercher and Tabakoff and the present study indicate that crossflow induced disturbance of the jet velocity profile has a diminishing effect on heat transfer. For $z_n/d \leq 0.5$, confined jet, $z_n/d = 0.25$, conditions begin to manifest. The larger increase in heat transfer found by Selvam et al.[8] when z_n/d was reduced from 0.96 to 0.5 is due to the increased wall velocity profile that results when confined jet conditions are approached. It is possible that the present data are underpredicted by the Kercher and Tabakoff[5] correlation because the correlation does not adequately predict the highly nonlinear effect of nozzle-to-target spacing as z_n/d approaches unity and because A_f is far outside the range studied by Kercher and Tabakoff. Consequently, the Kercher and Tabakoff correlation does not adequately describe the phenomena occurring in jet impingement arrays.

One unexpected phenomenon is the ring of low impingement flow about the orifices directly below the inlet tube. Figure 9 is a magnified photograph, (approximately 4×), of the grooved target surface after disassembly of the microjet array cooler. The photograph indicates, by the fine residue left on the target plate, that there was significant flow through the jet nozzles directly below the inlet tube and those jet nozzles greater than about one inlet tube diameter from the center. In the annular ring between these two areas is an area of low impingement flow. Because of the restriction that occurs in the plenum where the inlet flow must turn and expand radially through the plenum (Fig. 2), a low-pressure region exists above this annular ring of nozzles. Selvam et al.[8,9] confirmed this result numerically and showed that heat transfer is sensitive to plenum height. Their results showed a 17% reduction in heat transfer when the plenum height is reduced from the current 400 to 300 μm and a 19% increase in heat transfer when increased from 400 to 600 μm.

A correlation of the data was developed by starting with the general form of the analytical solution for local heat transfer below an impinging axisymetric jet[10,11]:

$$Nu_d = C Re_d^m Pr^n \tag{8}$$

where C, m, and n are constants. Variable properties are generally of concern in jet impingement heat transfer because the wall temperature can strongly effect the developing viscous and thermal boundary layers. Most researchers avoid the problem by maintaining a constant wall-to-jet temperature difference during experiments.

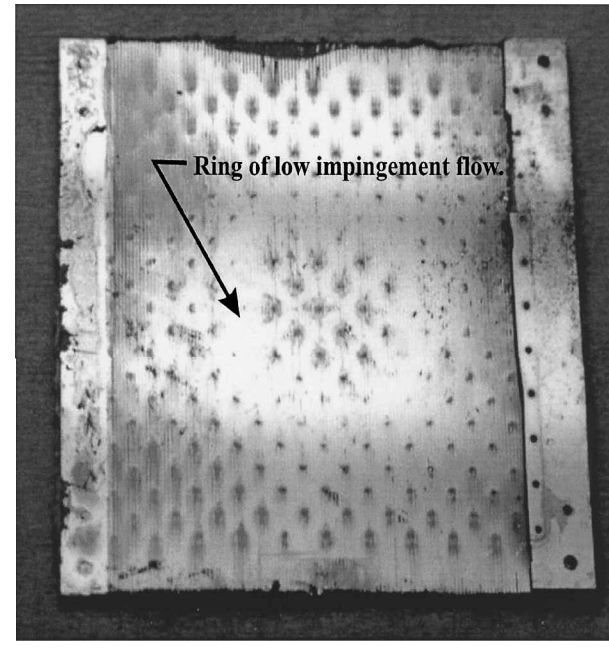

Fig. 9 Photograph of microjet cooler target plate.

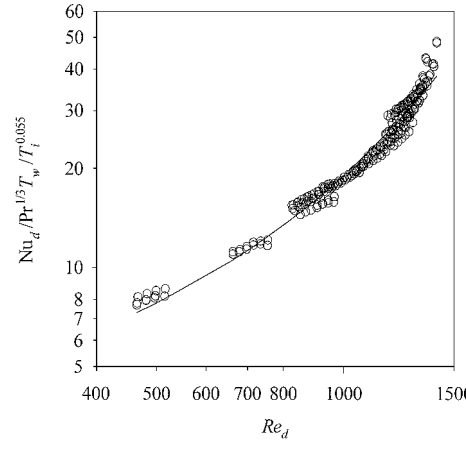

Fig. 10 Comparison of data to correlation, Eq. (8).

Kercher and Tabakoff[5] obtained the majority of their data for constant $T_w - T_i$ value of 41.7°C and some additional data for a $T_w - T_i$ of 83.3°C. This was done for the purposes of reducing measurement error and eliminating difficulties associated with variable properties. The present data were obtained for $0 \leq T_w - T_i \leq 53$°C because this would be more representative of an actual power electronics cooling application. Note that, in Fig. 1, the data for $T_w - T_i \geq 41.7$°C are distinguished from data obtained for lower temperature differences to make the effect of variable properties readily evident to the reader. It may also be seen that the effect of variable properties becomes more pronounced as Reynolds number increases. Variable properties are generally accounted for by introducing a term that includes the ratio of wall-to-bulk temperature or wall-to-inlet temperature. The authors found excellent results with both and chose the wall-to-inlet ratio because it is more readily available to the practitioner. Figure 1 also shows that Nusselt number Nu_d increases with Reynolds number at a rate greater than the power law rate. To encompass this effect, an additional Reynolds number term was added. The following correlation resulted:

$$Nu_d = 1.316 Re_d^{0.16} \exp(Re_d/637) Pr^{\frac{1}{3}} (T_w/T_i)^{0.055} \tag{9}$$

where the ratio T_w/T_i accounts for variable properties. The data are compared to Eq. (8) in Fig. 10. The correlation fits the data to within a mean absolute error of 5.6%.

Conclusions

High heat transfer rates have been obtained in a MEMS-based microjet array device using pressurized air as the coolant. Heat fluxes of over 15 W/cm^2 were obtained for $T_w - T_i$ of less than 50°C (or a T_w of only 72°C for ambient temperature air). Higher fluxes were not achieved because of the temperature limitation of the microjet array device.

The conclusions of Kercher and Tabakoff[5] are well supported by the current results, namely, that heat transfer increases with increasing A_f and heat transfer increases with decreasing z_n in the presence of crossflow.

The correlation of Kercher and Tabakoff[5] was found to significantly underpredict the current results. It is believed that the correlation does not adequately predict the performance of all combinations of array parameters that fall within the studied ranges. The numerical investigations in a companion work by Selvam et al.[8] show that the effect of jet-to-target spacing is highly nonlinear near the microjet array value of 0.96 mm. Although an extended surface target plate was employed to compensate for a value of A_f far outside the range of validity for Eq. (1), this change in geometry may have had the opposite effect.

An interesting flow phenomenon occurred in the jet array. An annular region of low impingement flow was observed on the target plate. The numerical work of Selvam et al.[8,9] show that a low-pressure region in the plenum caused low flow through the jets contained in an annulus around the target area of the inlet tube. Selvam et al.[8] further showed that heat transfer is sensitive to plenum height. The preceding conclusions indicate that there is still a need for a better understanding of array jet impingement heat transfer and a more generalized correlation.

Acknowledgments

This effort was supported by U.S. Air Force Laboratory funds. The authors wish to thank Richard J. Harris, University of Dayton Research Institute, for his diligent efforts in constructing the test apparatus and acquiring data. Kirk L. Yerkes's effort in arranging the fabrication of the microjet array device through Case Western Reserve University and the Defense Advanced Research Program Agency is also greatly appreciated.

References

[1] Leland, J. E., Price, D. C., Hill, B. P., and Collicott, H. E., "Cooling Down Hot New Electronics," *Aerospace America*, Vol. 33, No. 6, 1995, pp. 40–44.

[2] Livingood, J. N. B., and Hrycak, P., "Impingement Heat Transfer from Turbulent Air Jets to Flat Plates—A Literature Survey," NASA TM X-2778, 1973.

[3] Martin, H., "Heat and Mass Transfer Between Impinging Gas Jets and Solid Surfaces," *Advances in Heat Transfer*, Vol. 13, Academic Press, New York, 1977, pp. 1–60.

[4] Downs, S. J., and James, E. H., "Jet Impingement Heat Transfer—A Literature Survey," American Society of Mechanical Engineers, ASME Paper 87-HT-35, 1987.

[5] Kercher, D. M., and Tabakoff, W., "Heat Transfer by a Square Array of Round Air Jets Impinging Perpendicular to a Flat Surface Including the Effect of Spent Air," *Journal of Engineering for Power*, Series A, Vol. 92, No. 1, 1970, pp. 73–82.

[6] Kline, S. J., and McClintock, F. A., "Describing Uncertainties in Single-Sample Experiments," *Mechanical Engineering*, Vol. 75, Jan. 1953, pp. 3–8.

[7] "Heat Sinks 1996 Catalog," Wakefield Engineering, Wakefield, MA, 1996, p. 29.

[8] Selvam, R. P., Jung, Y., Khater, J., Ang, S., and Elshabini, A., "Computer Modeling to Optimize the Heat Removal Capacity of the Microjet Array," *Proceedings: 2001 International Symposium on Microelectronics*, International Microelectronics and Packaging Society, Reston, VA, 2001, pp. 616–621.

[9] Selvam, R. P., Khater, J., Leland, J. E., and Ponnappan, R., "Computer Modeling of Flow and Heat Transfer in a MEMS Based Air Microjet Array Impingement Cooling Device," *International Microelectronics and Packaging Society Proceedings: Window to the 21st Century in Microelectronics*, International Microelectronics and Packaging Society, Reston, VA, 1999, pp. 201–206.

[10] Liu, X., and Lienhard, J. H. V., "Liquid Jet Impingement Heat Transfer on a Uniform Flux Surface," *Heat Transfer Phenomena in Radiation, Combustion, and Fires*, Vol. HTD-106, 1989, American Society of Mechanical Engineers, New York, pp. 523–530.

[11] Liu, X., Lienhard, J. H. V., and Lombara, J. S., "Convective Heat Transfer by Impingement of Circular Liquid Jets," *Journal of Heat Transfer*, Vol. 113, No. 3, 1991, pp. 571–582.